Available online at www.sciencedirect.com
ScienceDirect
Journal of Sound and Vibration 307 (2007) 627–638
JOURNAL OF SOUND AND VIBRATION
www.elsevier.com/locate/jsvi

The detection of cracks in beams using chaotic excitations

J. Ryue*, P.R. White

Institute of Sound and Vibration Research, University of Southampton, Highfield, Southampton SO17 1BJ, UK

Received 30 December 2005; received in revised form 19 June 2007; accepted 20 June 2007
Available online 4 September 2007

Abstract

In the field of structural health monitoring (SHM), vibration-based SHM is one of the general approaches to detect and quantify damage to a structural system. Recently, progress has been made by using chaotic excitation signals and attractor-based analysis to detect damage in a structure. In this paper, a new approach for crack detection is explored by means of numerical simulations, using a chaotic signal as an input excitation and attractor-based measures. A cracked beam is modelled as a single degree of freedom piece-wise linear system whose stiffness is different during compression and expansion of the crack. To utilise this feature of the cracked beam, the single-phase portrait of the structural output is divided into two parts corresponding to the compression and expansion of the crack. Then the dissimiliarity between these two halves of the attractor are examined as a function of crack size. The measures introduced in this work are the half-space correlation dimension, which is the correlation dimension measured on one-half of the attractor, and the Hausdorff distance between the two attractors halves. For these two attractor-based measures, their variations are investigated with respect to crack size to find whether they are appropriate crack indicators or not.

1. Introduction

Vibration-based techniques provide powerful methods for structural health monitoring (SHM), allowing one to potentially detect and quantify damage. By quantifying changes in the responses of a structure, one may detect, locate or even diagnose the type of damage. Traditional techniques usually use broadband random signals to excite structures and investigate the changes in the modal parameters, e.g., modal frequencies, modal damping values and mode shapes [1–3]. Recently, progress has been made by using chaotic excitation signals and attractor-based analysis to detect damage in structures [4,5]. The fundamental characteristics of chaotic systems include sensitivity to changes in initial conditions, existence of positive Lyapunov exponents [6], and the system does not repeat its past behaviour (i.e., non-periodic). The fact that chaotic systems are sensitive to initial conditions implies that, in practice, one is unable to predict the long-term behaviour of a chaotic system, because a small change in the initial conditions leads to completely different long-term behaviour of the system. Chaotic dynamics are most easily understood when viewed from a phase space perspective, in other words, the attractor-based perspective. Therefore, attractor-based

*Corresponding author. Tel.: +44 2380 594930; fax: +44 2380 593190.
E-mail addresses: jr1@isvr.soton.ac.uk (J. Ryue), prw@isvr.soton.ac.uk (P.R. White).

0022-460X/$ - see front matter © 2007 Elsevier Ltd. All rights reserved.
doi:10.1016/j.jsv.2007.06.043

classification for the response of a structural system may be a useful approach, because the effect of damage is to alter the behaviour of attractors.

A variety of attractor-based metrics exist for the purpose of making quantitative statements about a dynamical system, e.g., correlation dimension [7] and Lyapunov spectrum [8]. For example, Craig et al. [9] have investigated the use of the correlation dimension for the condition monitoring of a bearing system with clearance which produces chaotic motion. Also, Todd et al. [4] have utilised phase space geometry changes resulting from damage incurred by a stiffness degradation in one spring of an eight degree of freedom system which is driven by a chaotic excitation signal. Since the structure acts as a 'filter' through which the chaotic signal is processed, small changes in the structure will serve to alter the degree to which the signal is filtered. Nichols et al. [5] have explored the utility of a chaotic excitation in an experiment by using nonlinear cross-prediction error [10] between damaged and undamaged attractors to detect damage simulated in a cantilever beam. These works and others have demonstrated that the attractor-based measures are effective features for quantifying the level of degradation to a given structure.

The work in this study is directed at exploring the feasibility of attractor-based methods using chaotic excitation to detect and identify cracks in a structure. As candidate crack indicators, two chaotic measures, i.e., the half-space correlation dimension and Hausdorff distance, are quantified for the response of a beam with a crack by means of numerical simulations. The correlation dimension is a measure representing global features of a system and conventionally an attractor in phase space has a single correlation dimension. Preliminary work [11] rapidly identified that correlation dimensions computed on the complete phase space provided an insensitive crack detection mechanism. Consequently, this work employs two correlation dimensions from a single phase portrait which are computed separately for motions associated with the compression and expansion of the crack in the beam. This local correlation dimension is referred to as the half-space correlation dimension.

The methodology discussed in this paper assumes that the beam is excited by a chaotic signal. The choice as to which chaotic system is used to generate this excitation is a relatively free one. There is no fundamental reason as to why any chaotic signal could not be used to design the excitation signal. Nevertheless, the use of a chaotic system with a symmetric attractor does offer an advantage. Specifically, the method looks for differences in the two halves of an attractor; if the excitation signal has symmetric attractor and the beam is not cracked then, at the output, the attractor will remain symmetric and our measures of difference between the attractor halves will be zero. If a system with an asymmetric attractor is used then the output generated by a beam with no crack will be non-zero. The methods described here could be used to monitor this value. However, there are no obvious benefits to be derived from using an asymmetric excitation, so the authors continue to exploit symmetric excitations. There are a large number of candidate systems, with symmetric attractors, that could be used to generate a suitable excitation. The authors have explored the use of a variety [11], but the results seem to be insensitive to the precise excitation system used. In the work reported here the authors only consider using the solution to Duffing's equation as an excitation.

In Section 2, an input chaotic signal and the two attractor-based measures are briefly introduced. In Section 3, the dynamical behaviour of a cracked cantilever beam is presented as an object structure for condition monitoring. Due to the presence of a crack, the beam structure possesses nonlinear characteristics. At low frequencies it can be modelled as a single degree of freedom (dof) piece-wise linear system which has different stiffnesses during stretching and compression of the crack. In Section 4, the half-space correlational dimension and Hausdorff distance are estimated from the attractor geometries of the structure output in phase space with different crack sizes.

2. Chaotic input signals and attractor-based measures

The chaotic solution of a forced Duffing equation will be applied as an input excitation force to a cracked beam in this study. The forced Duffing oscillator can be expressed as

$$\ddot{x} + c\dot{x} - k_1 x + k_2 x^3 = F\cos\omega t, \tag{1}$$

where c, k_1 and k_2 are system parameters of the Duffing oscillator, F is the amplitude of the forcing sinusoid and ω is the angular frequency of the forcing function. As shown in Eq. (1), Duffing's equation has a nonlinear

stiffness term proportional to x^3. The equation can be converted to a set of equations with three state variables, $x_1 = x$, $x_2 = \dot{x}_1 = \dot{x}$ and $x_3 = \omega t$:

$$\begin{aligned} \dot{x}_1 &= x_2, \\ \dot{x}_2 &= F\cos\omega t + k_1 x_1 - k_2 x_1^3 - c x_2, \\ \dot{x}_3 &= \omega. \end{aligned} \tag{2}$$

In a nonlinear system, there may be several attracting solutions corresponding to different initial conditions and system parameters. For instance, the time sequence of x_1 and the phase space trajectory produced by x_1 (displacement) and x_2 (velocity) exhibit a periodic solution if the parameters are set to $c = 0.05$, $k_1 = -0.53$, $k_2 = 1$, $F = 7.5$, $\omega = 1$ with initial values of $x_1(0) = 0$ and $x_2(0) = 0.4$. On the other hand, if the system parameter, k_1, is changed to $k_1 = 0$, the Duffing equation exhibits chaotic behaviour. The attractor for this set of parameters is shown in Fig. 1. It can be seen from this figure that chaotic signals establish complex and sophisticated attractor geometries in phase space and that they are non-periodic in the time domain.

There are several ways to quantify the geometrical complexity of chaotic attractors, which are fractal by nature. Most commonly, one seeks to use a dimension, such as the box-counting dimension, information dimension, correlation dimension to reflect the attractor geometry. The basic idea of the dimension of the chaotic system comes from the self-similarity, which does not simplify upon magnification. For details of these methods see Refs. [6,12].

The correlation dimension is a widely used measure quantifying chaotic systems since it is relatively easy to calculate. The concept of correlation dimension was introduced by Grassberger and Procaccia [7]. The correlation sum, $C(r)$, represents the number of point pairs $(\mathbf{x}_i,\mathbf{x}_j)$ whose distance in phase space is smaller than r and is expressed by

$$C(r) = \lim_{N\to\infty} \frac{2}{N(N-1)} \sum_{i=1}^{N} \sum_{j=i+1}^{N} U(r - |\mathbf{x}_i - \mathbf{x}_j|), \tag{3}$$

where N denotes the number of points in the attractor and $U(s)$ is the Heaviside unit step function, i.e., $U(s) = 1$ if $s>0$ and $U(s) = 0$ if $s<0$. The correlation dimension is defined by the logarithmic ratio between correlation sum $C(r)$ and the radius r as

$$D_c = \lim_{r\to 0} \frac{\log_2 C(r)}{\log_2 r}. \tag{4}$$

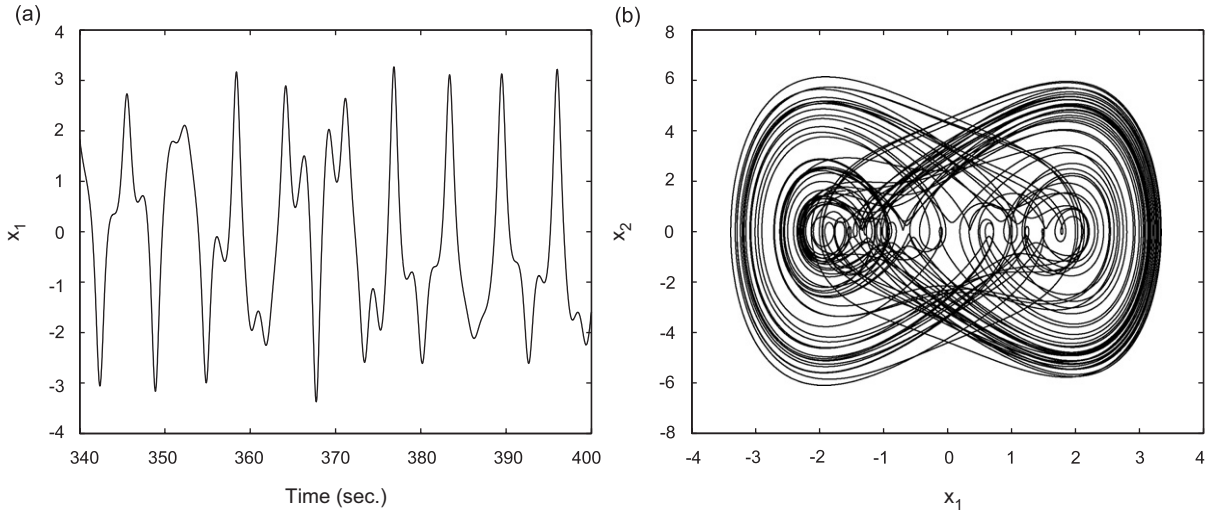

Fig. 1. The chaotic solution of the Duffing equation in Eq. (2) with $c = 0.05$, $k_1 = 0$, $k_2 = 1$, $F = 7.5$, $\omega = 1$, $x_1(0) = 0$, $x_2(0) = 0.4$ and $x_3(0) = 0$. (a) Time series of x_1. (b) Phase portrait projected onto the (x_1, x_2) plane.

The plot of $\log_2 C(r)$ versus $\log_2 r$ should contain a regime where the relationship is approximately linear and the slope there provided an estimate for the correlation dimension, since it implies that the attractor geometry appears to be self-similar under scaling.

The estimation of the correlation dimension, as defined by Eq. (4), from measured time series, can be accomplished using a variety of algorithms. The direct application of Eq. (4) imposes a computational burden proportional to N^2, where N is the number of samples in the time series. This can place excessive demands; accordingly efficient algorithms have been proposed [13]. In practical applications the estimation of correlation dimension from measured time series data is further hindered by noise and short data lengths. The effect is that it can be difficult to identify the linear region in the plot of $\log_2 C(r)$ versus $\log_2 r$. Much of the work on developing algorithms for estimating correlation dimension has set out to mitigate these problems. However, since simulated datasets are employed in this work, long data lengths can be simulated which contain (almost) no noise. Estimating the correlation dimension of such data is not particularly challenging and most of the existing algorithms are suitable. The optimised box-assisted algorithm, due to Grassberger [14], is the particular algorithm adopted here, primarily because it is simple and efficient. For the solution of Duffing's equation shown in Fig. 1, the estimated correlation dimension is 2.3, consistent with the values obtained in Ref. [15].

The Hausdorff distance is a measure of the similarity between two sets of points. It is expressed mathematically as

$$H(A,B) = \max\{h(A,B), h(B,A)\}, \tag{5}$$

where A and B denote two sets in space [16]. In Eq. (5), $h(A,B)$ represents the distance from set A to set B and is given by

$$h(A,B) = \max_{x\in A}\left\{\min_{y\in B}\{d(x,y)\}\right\}, \tag{6}$$

where x and y are points of set A and B, respectively, and $d(x,y)$ is the Euclidian distance between x and y. The Hausdorff distance represents the maximum minimum distance between two sets of data, or geometries, and is a measure of the similarity between them. For instance, if a set A is exactly equal to set B, then $H(A,B) = 0$. Fig. 2 illustrates an example of the Hausdorff distance between two sets. This example shows two sets of similar geometries but with different relative positions. It is clear from this example that $H(A_1,B_2)$ is shorter than $H(A_1,B_1)$, and hence the two sets A_1 and B_2 are more similar than the sets A_1 and B_1.

Consider the attractor of the Duffing equation as two attractors, which occupy the positive and negative half-planes of x_1, separately. The trajectories of this attractor projected onto the (x_1,x_2) plane constitute a symmetrical geometry about the origin, such that, if one of these two attractors is rotated about the origin, the two attractors become geometrically identical when $t \to \infty$ and so the Hausdorff distance between them will approach zero. For example, the Hausdorff distance computed for the Duffing system shown in Fig. 1, on the basis of 72,000 samples at a sample rate of 100 Hz, is 3.89×10^{-4}. This distance becomes smaller as $N \to \infty$ because the Duffing attractors are symmetric in phase space.

In order to quantify attractor-based measures from time series data, it is necessary to first construct its attractor geometry, called the phase portrait. To create the phase portrait, one should identify all the state variables of the object system. However, in most real situations, there is only a single-time series available. So,

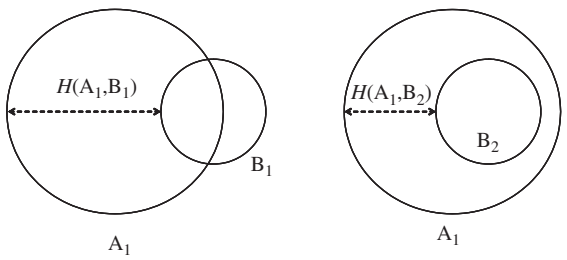

Fig. 2. An example of Hausdorff distances between two sets of circles with different relative positions.

one needs to reconstruct a pseudo-phase portrait which resembles the phase portrait of the original dynamical system. One can reconstruct an attractor in an n-dimensional pseudo-phase space by using delay coordinates from a single-time series, $v(t)$. That is, an n-dimensional delay vector, $\mathbf{x}(t) = \{v(t), v(t+\delta), \ldots, v(t+(n-1)\delta)\}$, creates a pseudo-phase portrait. Here δ denotes a suitably chosen time delay. In this reconstruction, the embedding dimension n should be greater than $2D_a$, where D_a is the dimension of the attractor [17,18]. For good attractor reconstruction, one needs to create an appropriate delayed vector by choosing an adequate delay time δ and embedding dimension n. There are several approaches for optimising the embedding parameters, n and δ, such as false nearest neighbours, autocorrelation functions, mutual information. Details of these methods for finding the minimum embedding dimension are summarised in Ref. [19].

Also another technique for phase space reconstruction is singular value decomposition (SVD), which was introduced by Broomhead et al. [20]. This method does not need one to consider the optimum delay time and the minimum embedding dimension separately and so makes the reconstruction easier. This is the method used in our work. For SVD, a trajectory matrix, $\mathbf{X} = [\mathbf{x}_1 \mathbf{x}_2 \ldots \mathbf{x}_N]^{\mathrm{T}}$ is created from a single-time series $v(t)$ using delay vectors of $\mathbf{x}_i = \{v(i), v(i+1), \ldots, v(i+(n-1))\}^{\mathrm{T}}$, where $i = 1, 2, \ldots N-(n-1)$. SVD of the trajectory matrix gives

$$\mathbf{X} = \mathbf{S}\boldsymbol{\Sigma}\mathbf{C}^{\mathrm{T}}, \tag{7}$$

where $\mathbf{S}$ and $\mathbf{C}$ are the eigenvector matrices of $\mathbf{X}\mathbf{X}^{\mathbf{T}}$ and $\mathbf{X}^{\mathbf{T}}\mathbf{X}$, respectively, and $\boldsymbol{\Sigma}$ is a diagonal matrix containing the singular values of $\mathbf{X}$. Eq. (7) can be written as $\mathbf{X}\mathbf{C} = \mathbf{S}\boldsymbol{\Sigma}$. The matrix $\mathbf{X}\mathbf{C}$ is the trajectory matrix projected onto the orthonormal basis $\{\mathbf{c_i}\}$, where $\mathbf{c_i}$ are the columns of $\mathbf{C}$. This method allows one to estimate the embedding dimesion n'. The dimension n' is acquired from the rank of the eigenvalue matrices, which is equal to the number of non-zero singular values. That is, if there are n' non-zero singular values in the matrix $\boldsymbol{\Sigma}$, this means that the matrix $\mathbf{X}\mathbf{C}$ with embedding dimension n' has no less information than the matrix with embedding dimension n.

For a cracked beam model used here, the SVD determined that there are only three non-zero singular values from output attractors with various crack sizes. That is, $n' = 3$. So the correlation dimensions are evaluated from the reconstructed attractors projected onto the three-dimensional space of $(\mathbf{c}_1, \mathbf{c}_2, \mathbf{c}_3)$. Here $\mathbf{c}_1$, $\mathbf{c}_2$ and $\mathbf{c}_3$ denote the first, second and third singular vectors of $\mathbf{X}$, normalised with respect to their singular values [21]. In the case of Hausdorff distances, they are estimated from the attractors projected onto the $(\mathbf{c}_1, \mathbf{c}_2)$ plane instead of $(\mathbf{c}_1, \mathbf{c}_2, \mathbf{c}_3)$ space to reduce computational effort. The reconstructed attractor in $(\mathbf{c}_1, \mathbf{c}_2)$ plane possesses sufficient geometrical structure to evaluate the differences between the two halves of the attractors.

3. Cracked beam modelling

The presence of a crack results in a beam having different properties in stretching and compression due to the discontinuity caused by a crack. That is, the structure can be regarded as a continuous system during compression. During stretching the material becomes discontinuous as the crack opens and the stiffness decreases, i.e.,

$$k_s = k - \Delta k, \tag{8}$$

where k is the stiffness of the homogeneous material and Δk is the stiffness difference of the material between compression (k) and stretching (k_s) [2]. Hence, if a beam has a crack, this system can be considered as a piece-wise linear system due to the nonlinearity of the stiffness arising because of the crack. For a cracked beam, it is assumed in this study that the stiffness ratio, $\Delta k/k$, is approximately equal to the relative crack size for small crack sizes [2,22]. That is,

$$\frac{\Delta k}{k} = \frac{\Delta l}{l} \quad \text{for } \frac{\Delta k}{k} \ll 1, \tag{9}$$

where Δl is the crack depth and l is the depth of the beam. It has to be noted that this linear relation is only valid for relatively small crack sizes, but these are the primary focus of this work.[1]

[1]Throughout this paper the relative crack size, $\Delta k/k$, is equated to the crack depth, $\Delta l/l$. For the larger crack sizes considered herein, this approximation may breakdown.

At low frequency, Bouraou et al. [2] modelled a cracked cantilever beam as a single dof mass–spring–damper system. This single dof beam model is applicable to the low-frequency response that is dominated by the first mode of the beam. Therefore, the forcing frequency has to be confined to this low-frequency region. The equations of motion of the cracked beam are expressed as

$$\begin{aligned} &\ddot{y} + 2\zeta_s\omega_s\dot{y} + \omega_s^2 y = F(t) \quad \text{for } y \geqslant 0, \\ &\ddot{y} + 2\zeta_0\omega_0\dot{y} + \omega_0^2 y = F(t) \quad \text{for } y < 0, \end{aligned} \tag{10}$$

where $\omega_s = \sqrt{k_s/m}$ is the natural frequency of the beam when it moves with the crack open (stretching), $\omega_0 = \sqrt{k/m}$ is the natural frequency of the homogeneous beam (compression), ζ is the damping loss factor, m is the mass of the beam. In these equations the subscripts '0' and 's' denote compression and stretching of the crack, respectively. For free oscillations, the ratio of the two oscillating frequencies of the cracked beam can be expressed based on Eq. (9) as

$$\frac{\omega_s^2}{\omega_0^2} = \frac{k_s/m}{k/m} = \frac{k - \Delta k}{k} = 1 - \frac{\Delta l}{l}. \tag{11}$$

If it is assumed that the damping factors are small and then $\zeta_s\omega_s \approx \zeta_0\omega_0$, the ratio of the damped oscillating frequencies $\omega_{s,d}$, $\omega_{0,d}$ depends on the crack size Δl as

$$\frac{\omega_{s,d}^2}{\omega_{0,d}^2} \approx \frac{\omega_s^2}{\omega_0^2} = 1 - \frac{\Delta l}{l}. \tag{12}$$

Therefore, the ratio of the natural frequency (ω_c) of the cracked beam to the natural frequency of the homogeneous beam (ω_0) can be expressed in terms of the relative crack size $\Delta l/l$ as

$$\frac{\omega_c}{\omega_0} = \frac{2(1 - \Delta l/l)^{1/2}}{1 + (1 - \Delta l/l)^{1/2}}. \tag{13}$$

Fig. 3 shows the dependence of frequency ratio, ω_c/ω_0 on the relative crack size of up to 0.5. The relative crack size of 0.5 is not small but is used in this figure to show the trend of how the natural frequency changes. As depicted in Fig. 3, the natural frequency of a cracked beam decreases with an increase of the crack depth. However, the variation of the natural frequency is relatively insensitive at small crack sizes which is the main area of interest in this study. For instance, when $\Delta l/l$ is smaller than 0.2, the reduction in the natural frequency is less than 5%. Variations in the natural frequency can be caused by a wide range of other mechanisms, such

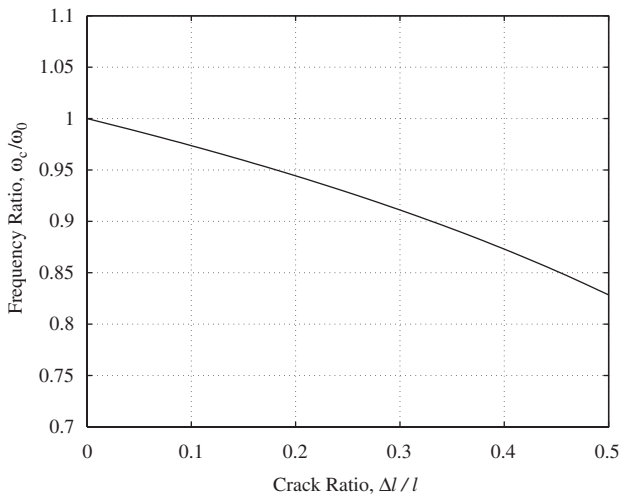

Fig. 3. The variations of the frequency ratio (ω_c/ω_0) of a cracked beam resulting from the relative crack size, $\Delta l/l$.

as temperature changes, boundary conditions, etc. Consequently, monitoring changes in the natural frequency is not a good indicator for cracks.

4. Attractor-based measures for crack detection

4.1. Attractor-based measures of a homogeneous beam

Prior to investigating the cracked beam, the correlation dimension and Hausdorff distance are examined for a single dof homogeneous beam in order to recognize whether chaotic properties of the input chaotic signal are preserved after passing through the homogeneous structure. To achieve this, the correlation dimension and Hausdorff distance are estimated from a homogeneous beam with various natural frequencies excited by a Duffing oscillator.

Fig. 4 shows an estimate of the power spectral density of the Duffing excitation shown in Fig. 1. From this it can be seen that the power of this signal is predominantly in a frequency band below 3 Hz, then the input bandwidth, f_{in}, was set to 3 Hz in this study. However, the span of the frequency band is tunable by scaling the time axis [5]. The natural frequency, f_0, of the homogeneous beam is varied to cover this input frequency range. Examples of normalised reconstructed phase portraits are illustrated in Fig. 5 for different resonance frequencies of the homogeneous beam. In this figure, $\mathbf{c}_1$ and $\mathbf{c}_2$ denote the first- and second-singular vectors of a trajectory matrix $\mathbf{X}$, normalised by their singular values. The effect of the natural frequency of the homogeneous beam on the correlation dimension and Hausdorff distance are shown in Figs. 6 and 7, respectively, plotted against normalised frequency.

Fig. 6 demonstrates that if the natural frequency of the homogeneous beam is greater than the upper frequency limit of the excitation signal, i.e., $f_0/f_{\text{in}} > 1$, the structural output will possess almost the same attractor geometry as the input excitation and the correlation dimension of the output approaches that of the input Duffing signal. On the other hand, if the natural frequency is placed inside the excitation frequency band, i.e., $f_0/f_{\text{in}} < 1$, then the correlation dimension tends to be increased as a result of structural filtering. The increase of correlation dimension for the lower natural frequencies may be interpreted as the attractor of the input Duffing signal, which has a sophisticated organisation in phase space, becomes more scattered in the embedding space due to the structural filtering. However, it was observed that the attractor is well structured at a much lower frequency $f_0/f_{\text{in}} = 0.1$ as shown in Fig. 5(a) and then the calculated dimension reduces again. This is because the low-frequency components of the input excitation signal dominate the structural output due to the low-natural frequencies of the structure.

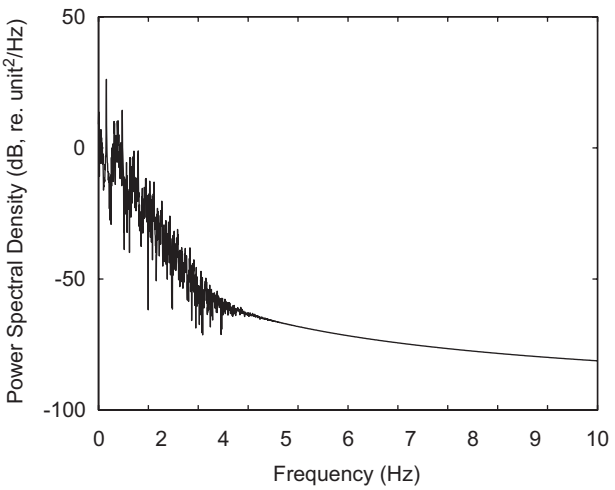

Fig. 4. Power spectral density of the input Duffing signal.

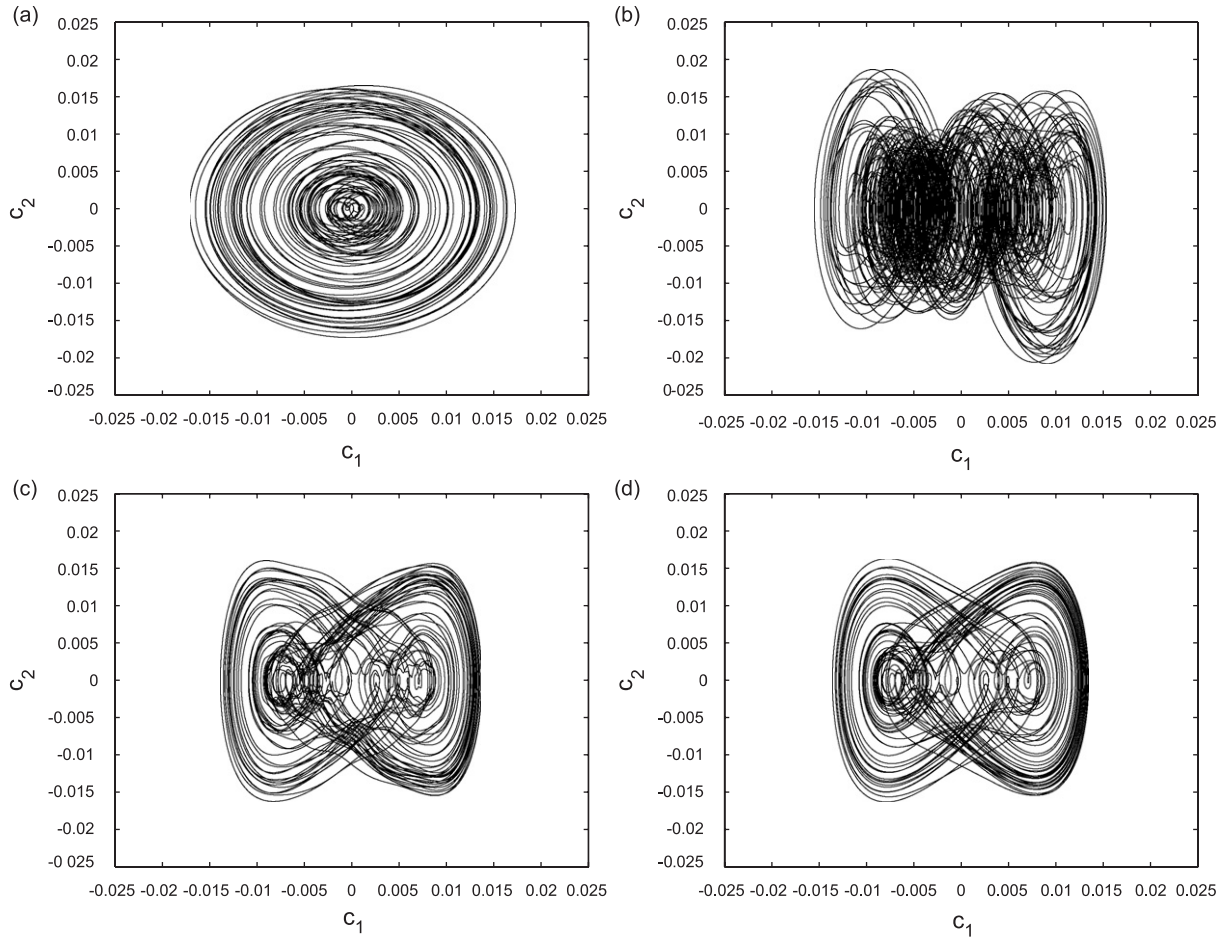

Fig. 5. Reconstructed attractors of the homogeneous beam model with different natural frequencies for the Duffing excitation in Fig. 1. (a) $f_0/f_{in} = 0.1$, (b) $f_0/f_{in} = 0.53$, (c) $f_0/f_{in} = 0.85$ and (d) $f_0/f_{in} = 1.17$.

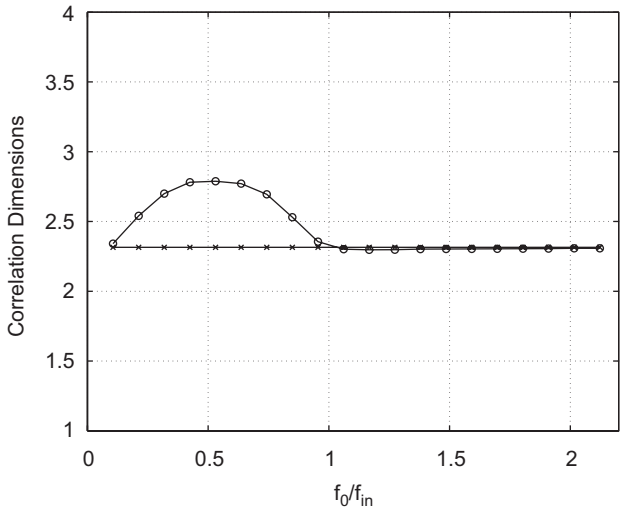

Fig. 6. Correlation dimensions of the input excitation, x_1 (×-marked line), and the output response, y_1 (○-marked line), corresponding to the natural frequency change of the homogeneous beam.

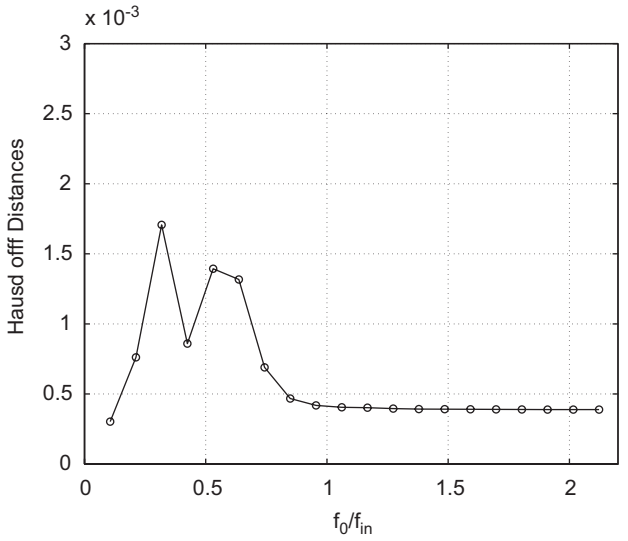

Fig. 7. Hausdorff distance of the output response, y_1, corresponding to the natural frequency change of the homogeneous beam.

Fig. 7 depicts the Hausdorff distance calculated for different natural frequencies of the homogeneous beam. It is seen from this figure that, like the correlation dimension, the Hausdorff distance approaches that of the input Duffing signal in case $f_0/f_{in} > 1$. If the data length is sufficiently long, the Hausdorff distance will tend to zero. But the finite data lengths ensure that non-zero Hausdorff distances are measured. In Fig. 6, the Hausdorff distance decreases in the low-frequency region.

Based on these two measures extracted from the output of the homogeneous beam, it is seen that if the natural frequency of the structure is higher than the band of excitation, the correlation dimension and Hausdorff distance of structure output is nearly the same as those of the input signal. Otherwise, these properties of the output differ from those of the input signal.

4.2. Attractor-based measures of a cracked beam

Half-space correlation dimensions and Hausdorff distances are estimated for two cracked beam models, which have frequency ratios of $f_0/f_{in} = 0.37$ and 5.2 in the absence of a crack. These two frequency ratios are chosen so as to locate the natural frequency of the beam outside and inside of the excitation frequency band. The crack in the beam opens when $y \geqslant 0$ (stretching) and is closed when $y < 0$ (compression).

For the cracked beam with $f_0/f_{in} = 5.2$, the normalised versions of the reconstructed phase portraits are illustrated in Fig. 8 for different crack sizes. The differences between the two estimated half-space correlation dimensions for the compression (D_c^-) and stretching (D_c^+) are depicted in Fig. 9 for a range of relative crack sizes. As shown in this figure, the difference between two half-space correlation dimensions is not sensitive to variations in the crack size. Therefore, this measure appears to be an inappropriate crack indicator.

The Hausdorff distance can be computed from the two halves of the attractor, one-half of the attractor has to be mapped to the other to account for the appropriate form of symmetry. For the cracked beam model with $f_0/f_{in} = 0.67$, Fig. 10(a) shows the variations of the Hausdorff distance corresponding to relative crack sizes. Whilst for the cracked beam model of $f_0/f_{in} = 5.2$, Hausdorff distances of output attractors are presented in Fig. 10(b) with respect to the relative crack size. Because the input chaotic signal is highly sensitive to changes in initial conditions, Hausdorff distances are evaluated for the three different initial values of $x_1(0) = 0.0$, 0.1 and 0.2 in order to assess the variability of the estimated Hausdorff distance caused by the effect of the initial condition. As shown in Fig. 10(b), it is clear that the Hausdorff distance gradually increases with relative crack size and gives consistent results for the three initial conditions on $x_1(0)$. Therefore, based on these results in Fig. 10, the Hausdorff distance of a cracked beam provides a consistent rise with a crack size for both cracked beam models.

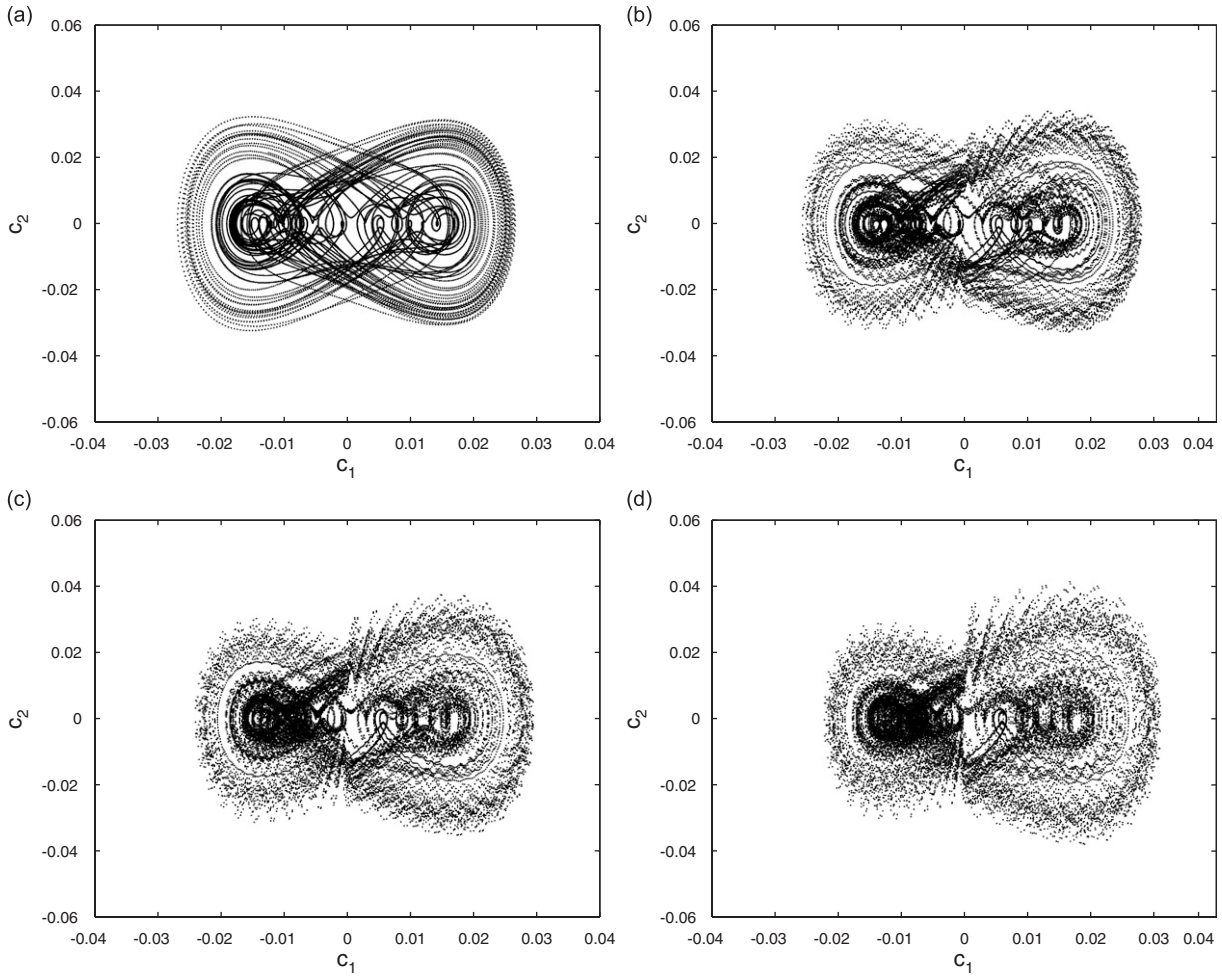

Fig. 8. Reconstructed attractors of the cracked beam model with $f_0/f_{in} = 5.2$, corresponding to different crack sizes for the Duffing excitation in Fig. 1. (a) $\Delta l/l = 0$, (b) $\Delta l/l = 0.1$, (c) $\Delta l/l = 0.2$ and (d) $\Delta l/l = 0.3$.

From these simulations, the differences between the two half-space correlation dimensions, in stretching and compression regions, were not sensitive to the relative crack size in the beam. The Hausdorff distance, however, gives monotonically increasing result with the relative crack size, especially for small crack sizes; a result which is robust to the natural frequency of the beam.

5. Conclusions

In this study, a new approach for crack detection was explored by means of numerical simulation, using chaotic signals as an input excitation and attractor-based measures. As candidate crack quantifiers, two attractor-based measures, i.e., the half-space correlation dimension and Hausdorff distance, were estimated in order to identify whether they are suitable crack indicators. For simplicity, a cracked beam was modelled as a single dof piece-wise linear system which has different stiffnesses during compression and stretching of the crack. As chaotic input forces, the solution of Duffing equation has been applied to the cracked beam. SVD has been used to reconstruct the attractor from time-series data.

Throughout this investigation, it has been shown that the half-space correlation dimension for stretching and compression region was relatively insensitive to changes in crack size in the beam. Therefore, the half-space correlation dimension is an inappropriate measure for identifying the relative size of a crack in beams. However, the Hausdorff distance continuously increases with the relative size of the crack. Hence, the

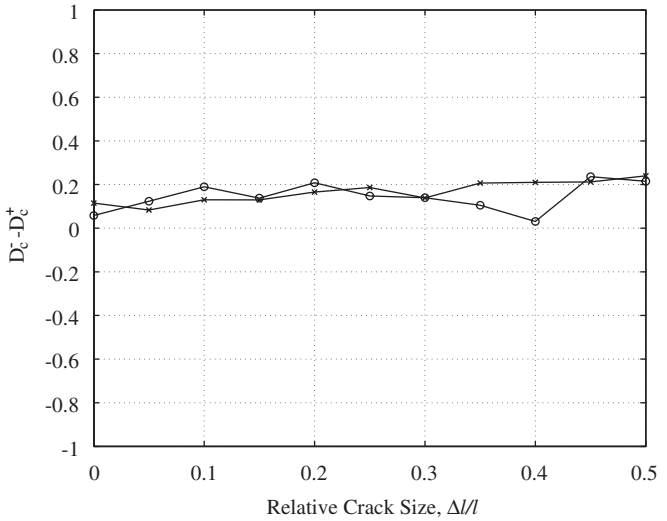

Fig. 9. Differences between the two half-space correlation dimensions at stretching and compression of the cracked beam models. ○-Marked line is for the model having $f_0/f_{in} = 0.67$; ×-marked line is for the model having $f_0/f_{in} = 5.2$.

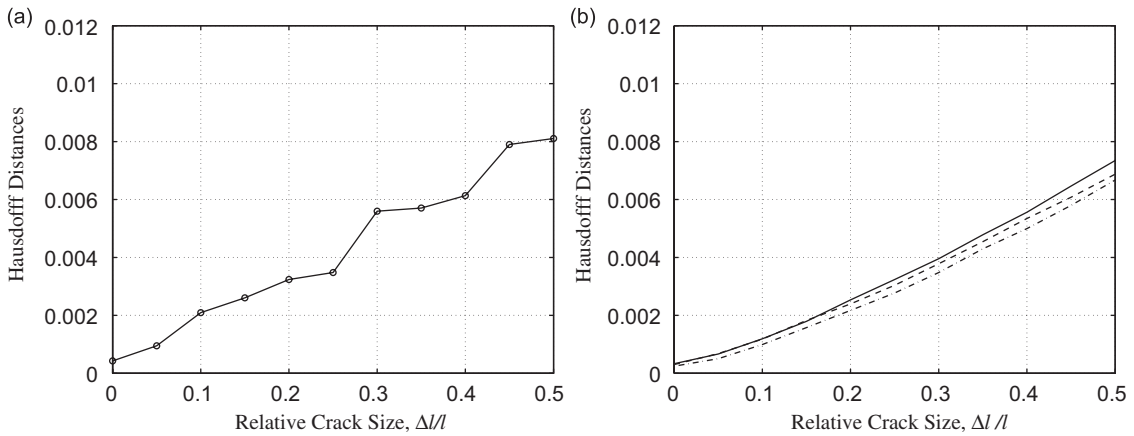

Fig. 10. Hausdorff distances corresponding to the relative crack size for the cracked beam model of (a) $f_0/f_{in} = 0.67$, (b) $f_0/f_{in} = 5.2$ with three different initial conditions of $x_1 = 0.0$ (the solid line), 0.1 (the dashed line) and 0.2 (the dash–dot line) for the Duffing excitation.

Hausdorff distance appears to be an adequate measure for quantifying the presence and size of cracks in structures. It should be noted that in order to obtain the Hausdorff distance which gradually increases with crack size, the length of output data needs to be long enough to reconstruct the attractors on a dense set of points. Furthermore, the Hausdorff distance was extracted from symmetric attractor geometries. There are, however, several chaotic signals which do not have symmetric trajectories in phase space and these are less suitable for this work. In addition, since issues of the crack location and the effect of noise in signals on the correlation dimension and Hausdorff distance were excluded in this study, more work is also necessary on these topics.

References

[1] A.K. Pandey, M. Biswas, Damage detection in structures using changes in flexibility, *Journal of Sound and Vibration* 169 (1999) 3–17.
[2] N. Bouraou, L. Gelman, Theoretical bases of free oscillation method for acoustical non-destructive testing, *Proceedings of Noise-Con97*, 1997, pp. 519–524.

[3] R.P. Sampaio, N.M.M. Maia, J.M.M. Silva, Damage detection using the frequency-response-function curvature method, *Journal of Sound and Vibration* 226 (1999) 1029–1042.
[4] M.D. Todd, J.M. Nichols, L.M. Pecora, L.N. Virgin, Vibration-based damage assessment utilizing state space geometry changes: local attractor variance ratio, *Smart Material and Structure* 10 (2001) 1000–1018.
[5] J.M. Nichols, M.D. Todd, M. Seaver, L.N. Virgin, Use of chaotic excitation and attractor property analysis in structural health monitoring, *Physical Review E* 67 (1–8) (2003) 016209.
[6] K.T. Alligood, T.D. Sauer, J.A. Yorke, *Chaos—An Introduction to Dynamical Systems*, Springer, Berlin, 1996.
[7] P. Grassberger, I. Procaccia, Measuring the strangeness of strange attractors, *Physica D* 9 (1983) 189–208.
[8] B. Brown, P. Bryant, Computing the Lyapunov spectrum of a dynamical system from an observed time series, *Physical Review A* 43 (1991) 2787–2806.
[9] C. Craig, R.D. Neilson, J. Penman, The use of correlation dimension in condition monitoring of systems with clearance, *Journal of Sound and Vibration* 231 (2000) 1–17.
[10] T. Schreiber, Detecting and analyzing nonstationarity in a time series using nonlinear cross predictions, *Physical Review Letters* 78 (1997) 843–846.
[11] J. Ryue, The Detection of Cracks in Beams Using Chaotic Excitations, MSc Thesis, ISVR at Southampton University, UK, 2004.
[12] E. Ott, T. Sauer, J.A. Yorke, *Coping with Chaos—Analysis of Chaotic Data and the Exploitation of Chaotic Systems*, A Wiley-Interscience Publication, John Wiley, New York, 1994.
[13] J. Theiler, Efficient algorithm for estimating the correlation dimension from a set of discrete points, *Physical Review A* 36 (1987) 4456–4462.
[14] P. Grassberger, An optimized box-assisted algorithm for fractal dimensions, *Physics Letters A* 148 (1990) 63–68.
[15] S.V. Nortely, Prediction of Epileptic Seizures from Depth EEG Signals, PhD Thesis, ISVR at University of Southampton, UK, 2002.
[16] M.F. Barnsley, *Fractals Everywhere*, second ed., Academic Press Professional, 1993.
[17] F. Takens, Detecting strange attractors in turbulence, *Lecture Notes in Mathematics*, No. 898, Springer, Germany, 1981.
[18] T. Sauer, J.A. Yorke, M. Casdagli, Embedology, *Journal of Statistical Physics* 65 (1991) 579–616.
[19] H. Kantz, T. Schreiber, *Nonlinear Time Series Analysis*, second ed., Cambridge University Press, Cambridge, 1991.
[20] D.S. Broomhead, G.P. King, Extracting quantitative dynamics from experimental data, *Physica D* 20 (1985) 217–236.
[21] K. Shin, Characterisation and Identification of Chaotic Dynamical Systems, PhD Thesis, ISVR at Southampton University, UK, 1996.
[22] L. Gelman, S. Gorpinich, Non-linear vibroacoustical free oscillation method for crack detection and evaluation, *Mechanical Systems and Signal Processing* 14 (2000) 343–351.